

Original Article

Using NARX Neural Networks to Advance Passive Radar Target Detection

Sattam Alkhurajji¹, Abir Alharbi²

^{1,2}Department of Mathematics, College of Sciences, King Saud University, Riyadh, Saudi Arabia.

²Corresponding Author : Abir@ksu.edu.sa

Received: 21 May 2025

Revised: 28 June 2025

Accepted: 13 July 2025

Published: 27 July 2025

Abstract - This study introduces a novel detection approach utilizing Artificial Neural Networks (ANNs) to enhance target detection with Passive Radar (PR) systems. The methodology goes through two distinct stages: primarily, a Backpropagation Neural Network (BPNN) to refine the target azimuth estimation, using the Levenberg-Marquardt algorithm as a replacement for the traditional MUSIC algorithm used in the classical methods. Subsequently, a NARX Recurrent Neural Network with time series features to collect data from prior flights is used to enhance detection capabilities in the proposed system. Training on datasets comprising 12 million data points from over 5000 flights demonstrated significant performance improvements, achieving a reduction in mean square error on a test flight of 1000 data points, with over 75% enhancement in localization accuracy compared to classical passive radar systems.

Keywords - Artificial neural networks, Backpropagation neural networks, NARX, Recurrent neural network, Passive Radar, Azimuth angles.

1. Introduction

Passive radar (PR) usage as a surveillance tool has been gaining popularity lately. Unlike traditional active radar systems, which emit their own signals, PR relies on external sources, such as telecommunications transmitters, such as commercial broadcast transmissions (radio, TV, and Cellular), to detect and track moving objects like vehicles and aircraft. PR brings cost-effective and environmentally friendly benefits, as it does not generate electromagnetic pollution, and allows for installations across multiple locations, enhancing target monitoring capabilities¹. Improving PR systems' effectiveness is very much needed, and research in this field is low, while PR technology is very beneficial in areas of stealth and security in military applications, environmental monitoring, air traffic control, and maritime surveillance.

Though PR system improvement is desirable in many fields, the inherent complexity and unpredictability of the electromagnetic environment face challenges for conventional target detection methods. Traditional geometric approaches often struggle to adapt to the dynamic nature of moving targets². In contrast, machine learning and artificial intelligence techniques have shown competitiveness in finding solutions to these challenges in similar domains. Recent literature highlights advancements in improving PR performance through machine learning applications, such as the work by Xiaoyong Lyu and Jun Wang, "Direction of arrival estimation in passive radar based on deep neural network",³ which uses deep neural networks for estimating direction of arrival that greatly affects PR accuracy. There is also a paper by Li Song et al., entitled "Radar track prediction method based on BP neural network",⁴ where backpropagation (BP) techniques were employed for improving radar detection. Another group lead by Mohammed Khalafalla et al. enhanced Radar localization capabilities by a hybrid novel method in "Two-Dimensional Target Localization Approach via a Closed form Solution Using Range Difference Measurements Based on Pentagram Array"⁵. Some research papers in the area of singular value decomposition (SVD), like Ali Noroozi et al., "Target Localization in Multi-static PR Using SVD Approach for Eliminating the Nuisance Parameters",⁶ showed good results in improving the accuracy properties of the method with the Cramer-Rao lower bound (CRLB) for target localization, and they developed BR-based localization to compare to the hyperbolic localization derived from range difference measurements. Other methods approach the PR detection problem as a classification problem and build a classifier with machine learning methods, such as the support vector regression⁷, multi-task autoencoder⁸, and the multilayer perceptron (MLP)⁹.



In this research, the aim is to introduce a novel approach that is based on artificial intelligence capabilities, which differs from traditional SVD and basic MLP methods found in the literature, and help advance the critical field of Passive Radar systems in order to improve their functionality, and hence increase the benefits of better surveillance and security to end users. The approach consists of two stages.

In the first stage, classical geometric calculations (MUSIC algorithm) are replaced by BP-NN (Back propagation neural networks) techniques for accurate azimuth estimation. Furthermore, in the second stage, the target detection is enhanced by an NARX (Nonlinear Autoregressive Network with Exogenous Inputs) network employing historical target data to optimize PR system detection performance. The proposed methodology in this research combines two neural network techniques that have not previously been applied to enhance Passive Radar systems. We believe this approach represents a significant step forward in advancing this field.

2. Passive Radar

Passive Radar detection relies on comparing direct signals from transmitters with echoes reflected off targets. This system typically needs at least two receiving channels, where one acts as a reference for the original signal by aligning a directional antenna towards the transmitter. The second antenna monitors the target area and captures echo signals for processing. PR measures the time difference of arrival between the direct and reflected signals, enabling the calculation of bistatic range and Doppler shifts and the direction of arrival. In passive radar systems, the key measurement is the bistatic range, defined as the difference in distance between the paths from the transmitter to the target and from the transmitter to the receiver. Points that maintain a constant bistatic range form an ellipsoidal shape, with the transmitter and receiver serving as the foci of the ellipse. Additionally, the Doppler shift observed in passive radar is directly related to the bistatic velocity, which indicates how quickly the bistatic range alters.

The angle formed by the target, transmitter, and receiver, known as the bistatic angle, is crucial for calculating target localization, and involves determining the intersection of multiple bistatic ellipsoids derived from various transmitter-receiver pairs. The estimation of direction of arrival (DOA) is crucial in passive radar, and it uses antenna arrays across different spatial regions to capture signals from multiple angles. Through advanced signal processing techniques in traditional systems, the radar system can determine azimuth angles that are essential for effective tracking and surveillance, hence improving PR functionality. Therefore, improving PR functionality is dependent on accurate bistatic range measurement and precise Azimuth estimation values, which are explained in detail in the following sections.

2.1. Bistatic Range

Target positioning can be achieved by integrating data on bistatic range and direction of arrival, mirroring techniques found in traditional monostatic radar systems, but this approach may lead to occasional inaccuracies; therefore, other geometric methods must be applied. In this research, as can be seen in Fig. 1, the transmitter is at $Tx(x_1, y_1, z_1)$ and the receiver is at $Rx(x_2, y_2, z_2)$, while if there is a target flying at the point $(x(t), y(t), z(t))$ with an angle formed between the target-transmitter and target-receiver paths referred to as the bistatic angle (β), then the distances can be expressed mathematically using the following equations:

$$\begin{aligned} d_1(t) &= \sqrt{(x_1 - x(t))^2 + (y_1 - y(t))^2 + (z_1 - z(t))^2} \\ d_2(t) &= \sqrt{(x_2 - x(t))^2 + (y_2 - y(t))^2 + (z_2 - z(t))^2} \\ d_b &= \sqrt{(x_2 - x_1)^2 + (y_2 - y_1)^2 + (z_2 - z_1)^2} \end{aligned} \quad (1)$$

Where $d_1(t)$ represents the distance from the transmitter to the target, $d_2(t)$ denotes the distance from the target to the receiver, and d_b signifies the baseline distance from the transmitter to the receiver. Hence, the variation between the indirect path $d_1(t) + d_2(t)$ and the direct path d_b is called the Bistatic Range, given by:

$$d(t) = d_1(t) + d_2(t) - d_b \quad (2)$$

and also, can be calculated from the measured delay τ between the reference and echo signals, by $R = c \tau$, with speed of light $c = 3 \times 10^8$ m/s.

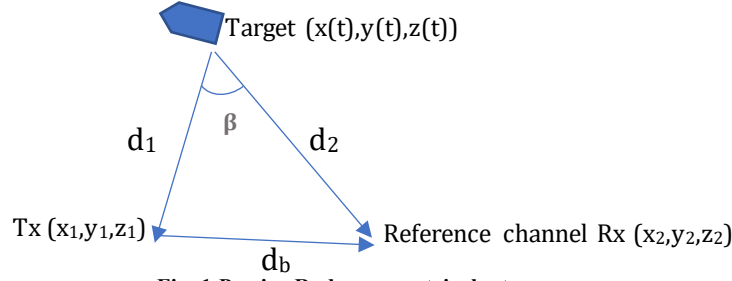


Fig. 1 Passive Radar geometrical setup

2.2. Azimuth Values

In PR systems, estimating the direction of arrival (DOA) is essential for effective array signal processing and target detection. This estimation involves using an array of antennas positioned in various spatial locations to capture signals from different sources. By applying advanced signal processing techniques, the system can determine the direction of these incoming signals and calculate the corresponding azimuth angle. Azimuth is the angle in the horizontal plane that a line or vector makes with a reference direction or the path of a wave (e.g. sound wave or radio wave) and is used for indicating the direction of an object, relative to a point. PR records reflected targets' signals, and multiple antenna deployments might greatly improve detection capability.

The time difference of arrival (TDOA), which is also a well-known method of localization measures the difference in time it takes for a signal to arrive at several other antennas. Meanwhile, the arrival times at each antenna (AOA) and the phase difference between signals received from different antennas can be used to calculate the azimuth angle according to the principles of interference. Various algorithms are available for DOA estimation, including techniques like MUSIC (Multiple Signal Classification) and ESPRIT (Estimation of Signal Parameters via Rotational Invariance Techniques). These algorithms analyze the incoming data to accurately compute azimuth angles, thereby improving the overall effectiveness of passive radar systems¹⁰.

The MUSIC algorithm operates on the principle of performing characteristic decomposition on the covariance matrix derived from the array output data. This process results in two orthogonal subspaces: one representing the signal components and the other representing noise. These two subspaces are then used to construct a spectral function. Hence, if two antennas are spaced apart by a known distance dd , and the arrival times at each antenna are denoted as $T1$ and $T2$, the azimuth angle can be calculated using the speed of light c . The relationship can be expressed mathematically to determine the azimuth angle based on these parameters

$$azimuth = \tan^{-1} \left[c \frac{(T1 - T2)}{dd} \right]$$

Hence, with azimuth calculation using these parameters, the system can determine the direction of a target, which is essential for tracking and surveillance applications.

In this research, a PR system with eight CFF antennas is utilized to collect signals and estimate the Azimuth using a Backpropagation Neural Network (BP-NN) instead of the traditional MUSIC algorithm built in the PR system. Hence, the signals from the eight antennas are collected, processed, and used to approximate the Azimuth angle through stages of training and learning in the BP-NN. Secondly, this newly computed azimuth angle approximation is used in a NARX (Nonlinear Autoregressive Network with Exogenous Inputs) recurrent neural network to detect targets. This novel hybrid technique of BB-NN and NARX-NN has not been used in the PR research field, but according to our preliminary results, it has achieved a very promising improvement in the performance of PR systems.

3. Backpropagation Neural Net

Backpropagation algorithm (BP) is the most reliable neural network used by researchers to solve many nonlinear function approximations effectively. BP trains the neural network through different training algorithms depending on the problem's features, and it updates the weights in its learning phase through updating equations that take into account the error scored in the previous step¹¹. In simple terms, after each forward pass through a network, backpropagation performs a backward pass while adjusting the learning weights, according to the difference between its target estimation and the true target value. The BP network has several layers depending on its architecture design, and each layer applies a suitable activation function to calculate the final

output values. The network can have various numbers of layers within the network, which represent the depth of the network; these inner layers are called hidden layers. Each layer, l , also has a width which represents the number of nodes it includes, as seen in Fig. 2.

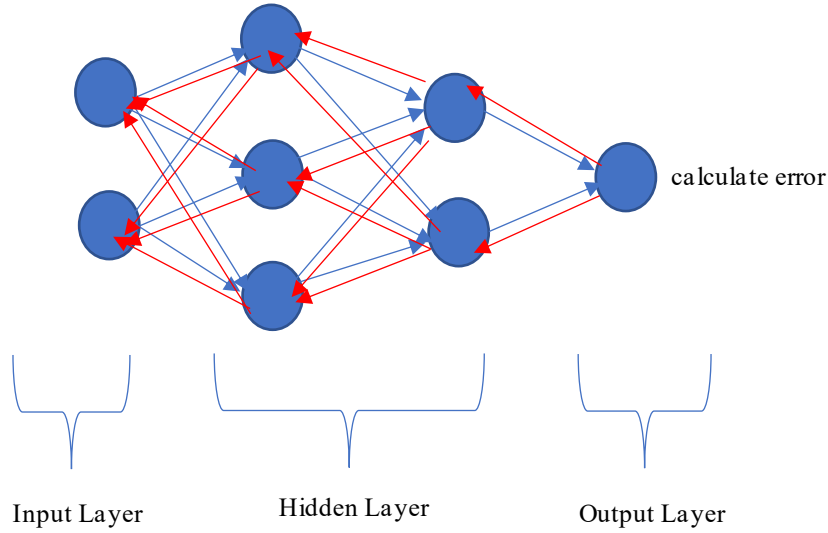


Fig. 2 Backpropagation Neural Net with two hidden layers
(showing an example error path propagating back to the input layer in red)

3.1. The Levenberg–Marquardt Algorithm

There are many learning algorithms available for the learning phase in a BP network. one of these learning algorithms is the Levenberg–Marquardt (LM) algorithm, which aims to minimize a function $E(w)$, which is typically the sum of squared errors between the predicted output y and the actual output t ¹²:

$$E(w) = \frac{1}{2} \sum_{i=1}^N (t_i - y_i(w))^2 \quad (3)$$

Where w represents the weight vector of the neural network, and N is the number of data points. The update equation for the weights w in the LM algorithm is given by:

$$w^{k+1} = w_k - (J^T J + \lambda I)^{-1} J^T e \quad (4)$$

Where J is the Jacobian matrix of the network's error function with respect to the weights, and the following parameters:

- e is the vector of defined errors,
- λ is a damping parameter
- I is the identity matrix.

The LM algorithm works by iteratively updating the weights of the neural network according to its updating equation given in Eq. 4. Notably, in the LM algorithm, when the parameter λ is large, the update equation is similar to the Gradient Descent method. On the other hand, when λ is small, the updating equation of the LM algorithm is similar to the Gauss-Newton method. Hence, the value of λ is dynamically adjusted at each iteration through appropriate equations. These equations take into account the following:

- If the error decreases, λ is reduced, making the method faster.
- If the error increases, λ is increased, making the method more robust¹².

The main advantages of the LM algorithm are its speed of convergence compared to other optimization algorithms like Gradient Descent, its stability in handling ill-conditioned problems, and its capabilities to adapt to the dynamics of the problem through damping λ . These properties make the LM algorithm particularly suitable for training medium-sized neural networks in various applications such as curve fitting, function approximations, optimization, system identification, and time-series prediction¹⁴, which is needed in PR systems.

4. NARX Neural Network

NARX is a Nonlinear Autoregressive Network with exogenous inputs and is a type of recurrent neural network (RNN) specifically designed for modeling time series data. Unlike traditional feedforward neural networks, NARX networks incorporate feedback loops, making them effective for tasks where the current output depends on previous outputs and external inputs or a time series of inputs¹³. Multi-step-ahead prediction and dynamic modeling are much more complex to deal with than one-step-ahead prediction. Several recurrent neural networks have shown competitiveness with traditional methods and the ability to model and find acceptable solutions in these complex tasks. The NARX recurrent networks forecast the future output time series values by utilizing the previous values of the same endogenous series and the previous values of the exogenous series.

4.1. NARX Architecture

The NARX model time series can be mathematically represented as ¹³:

$$y(t) = F(y(t-1), y(t-2), \dots, y(t-n), u(t-m)) \quad (5)$$

- $y(t)$ is the output at time t .
- $u(t)$ represents the exogenous inputs.
- F is a nonlinear function.
- n and m are the memory orders for the outputs and inputs, respectively.

NARX-NN has a multilayer structure consisting of an input layer that takes past output values and current exogenous inputs, a hidden layer that captures the nonlinear relationships in the problem and finally an output layer that provides the predicted values for future time steps. Since the target output is available during the training of the network, a series parallel architecture is created, in which the target is used instead of feeding back the estimated output, as shown in ¹⁵:

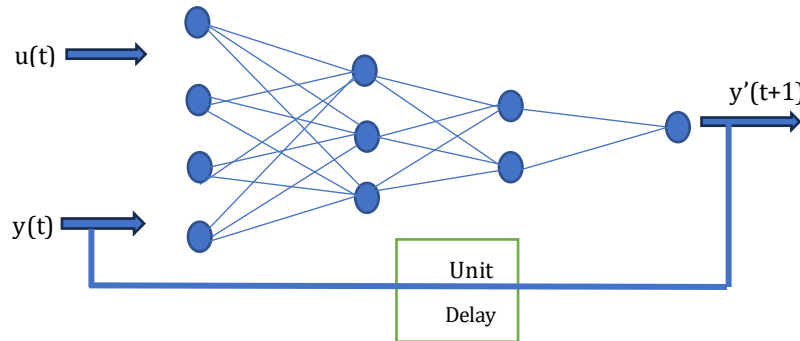


Fig. 3 Time series architecture

4.2. NARX-NN Key Features

NARX-NN has many advantages, the most relevant to this research is the ability to model linear and nonlinear phenomena and find dynamic predictions which are effective for time-dependent data, in addition:

- NARX incorporates past values of the output variable, allowing it to capture complex temporal dynamics, known as nonlinear autoregression.
- NARX incorporates external variables or exogenous inputs to provide a more comprehensive and accurate modeling approach.
- NARX architecture typically includes a feedback loop, where the output from previous time steps is fed back into the network, gaining extra predictive capabilities.

In general, the weights and biases of the NARX network are randomly chosen, and the activation functions for the hidden and output layers are set by default to the hyperbolic tangent activation function (tansig) during the training phase. NARX has proven useful in various fields, including finance, engineering, and all fields of science or environmental science, for tasks like forecasting and system identification. NARX has previously been applied by many researchers to model nonlinear processes. Coruh et al.¹⁴ applied NARX to predict the adsorption efficiency percentage for the removal of zinc ions from wastewater. Lin et al.¹⁵ have also mentioned NARX network capabilities as a powerful modeling and validation tool with much faster convergence and more efficient than other neural network models.

5. Data Collection and Procedure

Flight data to train the network was obtained from the PSATRI research center at King Saud University, which has a passive radar system and has collected local flight data for years. The sample dataset consisted of 32 parameters, with the first 16 parameters consisting of PR Track Raw bistatic and velocity, PR Track detection frequency, PR Track Raw Azimuth, PR Track bistatic Range and Velocity, PR Track Filtered Azimuth, PR Track Range, and PR Track X-coordinate, PR Track Y-coordinate. Additionally, ADSB recorder data was collected from the flying plane target, which consists of: ADSB bistatic Range and Velocity, ADSB Track Range, ADSB Track Azimuth, ADSB Track X-coordinate, and ADSB Track Y-coordinate. These ADSB data parameters were used as the true target inputs during the training. The last 16 columns in the data matrix consisted of the coefficients collected from 8 CCF antennas mounted around the PR system. The data was split randomly into 70% for training, 15% for validation, and 15% for test sets.

5.1. First Phase: Azimuth Estimation

In this phase, there were 19 variables entering into the BP-NN algorithm as input units, chosen from the dataset parameters:

- 1) PR Track Detection Frequency channel.
- 2) PR Track Raw Bistatic Range.
- 3) PR Track Raw Bistatic Velocity.
- 4) $CCF[n].x$, for $n = 0, 1, \dots, 7$ (coefficients from 8-antennas)
- 5) $CCF[n].y$, for $n = 0, 1, \dots, 7$ (coefficients from 8-antennas)

The BP-NN acted as a function approximation and was trained by a Levenberg-Marquardt algorithm, with two hidden layers and 10 hidden units in the hidden layer and (tansig) activation function, and the true target data set was the ADSB Track Azimuth. The output of the BP-NN gave an accurate estimation of the Azimuth in degrees ($-360^\circ \leq \text{Azimuth} \leq 360^\circ$) for each point in the flight. In fact, when compared to the ground truth in ADSB Track Azimuth, the BP-NN Azimuth values were 90% more accurate than the PR Azimuth MUSIC algorithm calculations previously used by the research center.

5.2. Second Phase: Target Detection

In phase two of this research methodology, there are 4 parameters that are entered as inputs in the NARX-NN stage:

- 1) The azimuth value output from phase one
- 2) PR Track Bistatic Range.
- 3) PR Track Bistatic Velocity.
- 4) PR Track Range.

With the outputs in this network being a 2-dimensional space, Cartesian coordinates (x, y) , representing the approximation location target, with the true target dataset coming from ADSB Track X-coordinate and ADSB Track Y-coordinate. A NARX-NN with 15 hidden layers, each with 10 hidden units, and three previous flight locations acted as inputs for the time series ($\text{Lag}=3$). The Levenberg-Marquardt algorithm was utilized in the NARX-NN learning phase, and the mean squared error (MSE) was used to measure performance in training, validation, and testing datasets.

In this research, two experiments were conducted, each using a dataset of different sizes: 8 million flight points and 12 million flight points. It was noted in these trials that providing large sets of flight data has helped greatly in the algorithm training stage and that the NARX recurrent neural networks' time series features have helped capture the dynamics in the target detection process needed to reach reliable, optimistic results.

6. Results and Analysis

6.1. Experiment 1

A dataset consisting of 8 million data recordings in more than 2500 flights was used. Phase one was first initiated, and after 76 epochs, the estimated azimuth values were obtained with accuracy $\text{MSE}=0.0561$. Fig. 4 shows the accuracy of the phase 1 azimuth estimation function approximator. Phase two is then activated with the updated input values, and the Best Validation Performance was reached at epoch 260 of NARX-NN, with a mean squared error $\text{MSE}=44.2$.

Figure 5 shows all errors coming from the training, validation, and testing datasets decreasing throughout the epochs. A selected flight with 1000 points was extracted prior to running the network and was not part of any of the training, validation and testing datasets for location detection and testing of the trained NARX system (a flight data set is fixed for all comparisons). Figure 6 shows a comparison of the Cartesian and polar plots of the flight with both the NARX-NN and true ADSB locations.

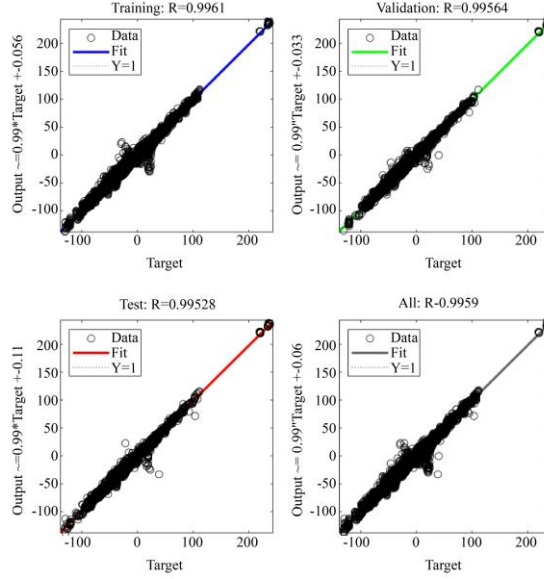


Fig. 4 Phase 1. Azimuth values through function approximation

As can be seen in Fig. 7, the plots of the NARX-NN results compared with the classical PR system locator and the ADSB true location, clearly, the NARX-NN results are superior to the PR system, which scored an MSE of MSE 177.18.

6.2. Experiment 2

A dataset consisting of 12 million-point recordings coming from more than 5000 flights was used for training the NARX-NN, and the results have improved with the Best Validation Performance reached at epoch 997 and MSE=33.3. Fig. 8 shows all errors coming from the training, validation, and testing datasets decreasing throughout the epochs. The NARX-NN was tested on the same selected flight with 1000 points, resulting in the comparison of both Cartesian and polar plots shown in Fig.9. As can be seen in Fig. 10, comparing the plots of the NARX-NN and classical PR system prediction and the ADSB true location, the performance has improved by over 75 %. With more training flights provided in the dataset, the artificial neural network was able to train and learn and hence improve its accuracy in target localization.

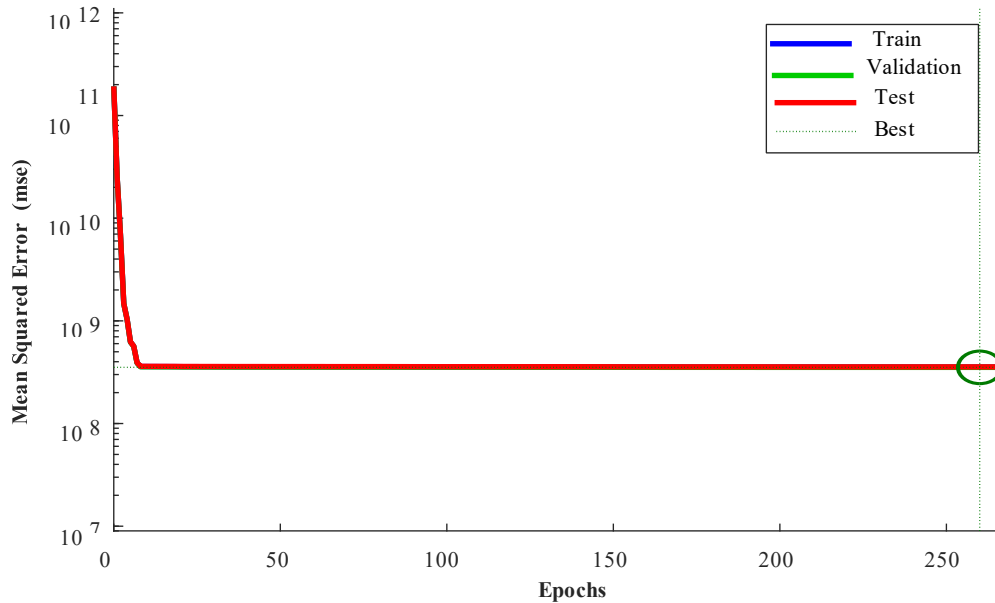


Fig. 5 Experiment 1- Performance of NARX-NN by error plots

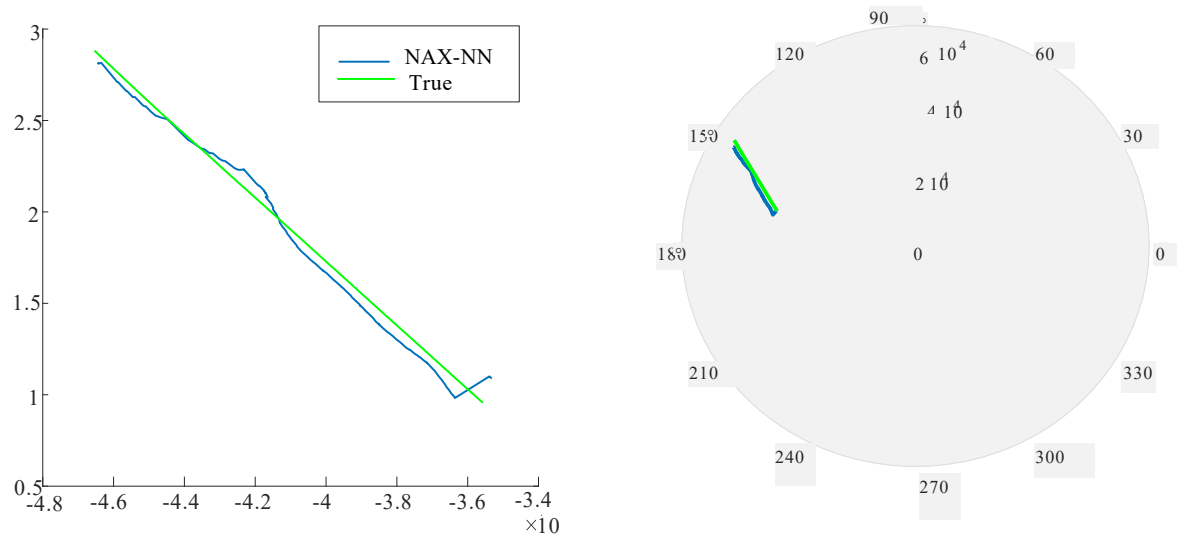


Fig. 6 A selected flight location detection in Cartesian and polar form

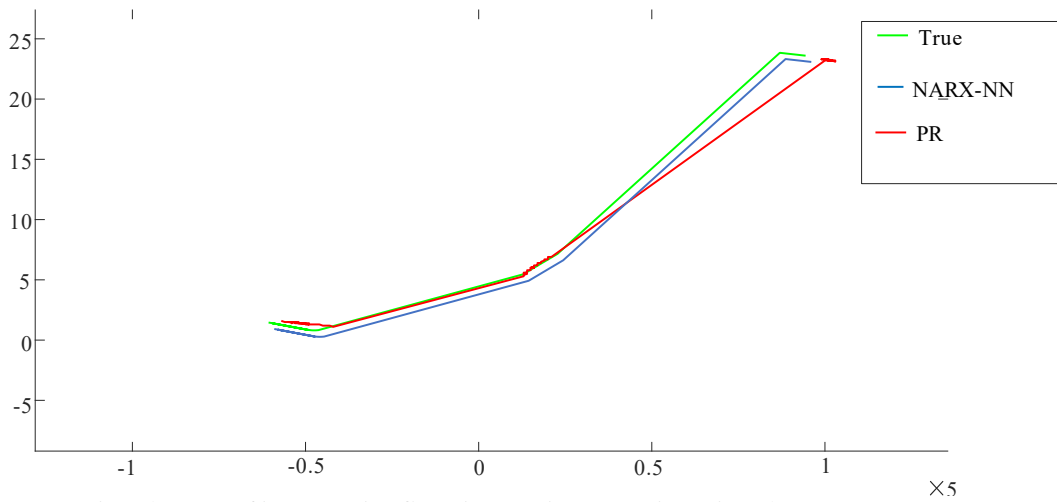


Fig. 7 A selected flight detection Cartesian location comparison with NARX, True and PR system

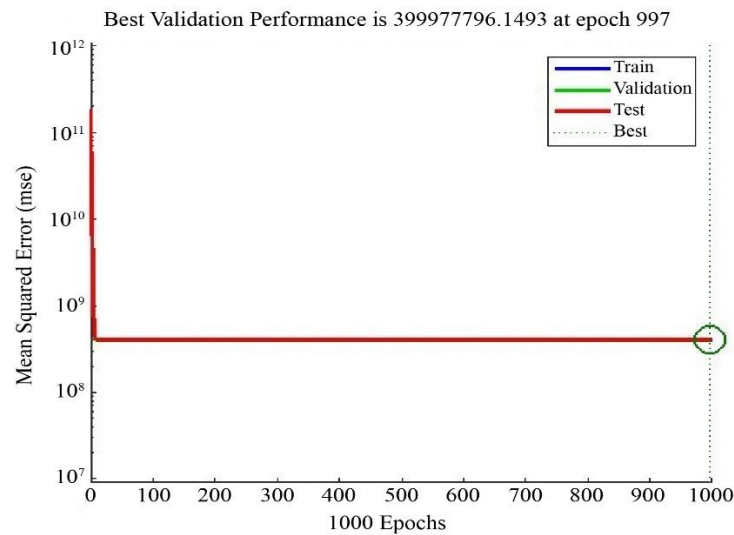


Fig. 8 Experiment 2 -performance of NARX NN errors plot

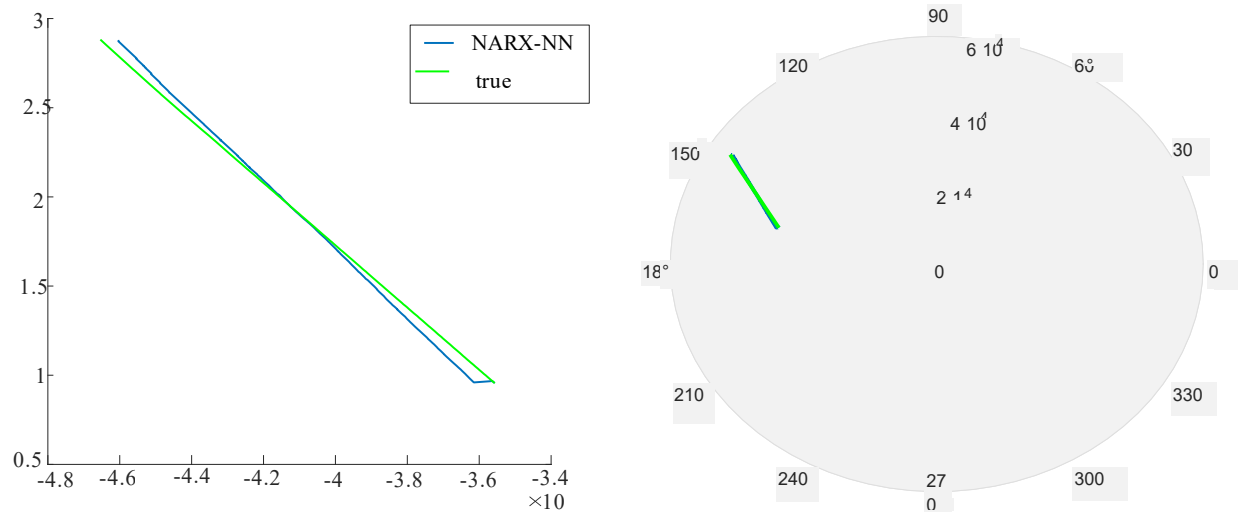


Fig. 9 A selected flight location detection in Cartesian and polar form

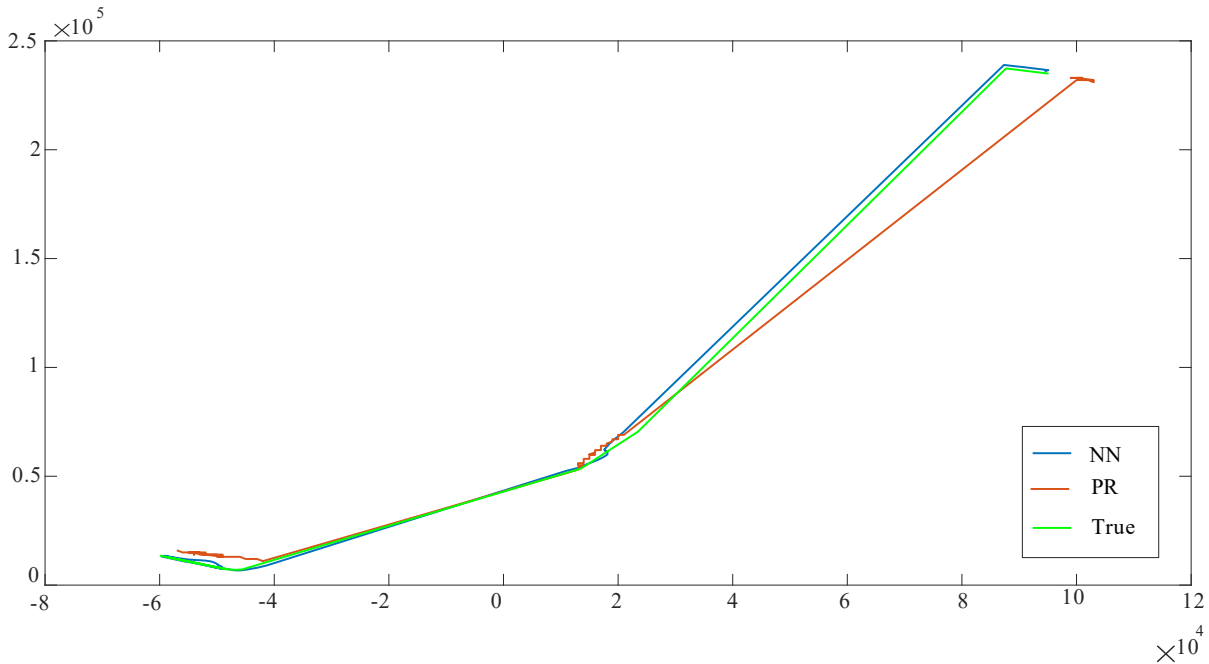


Fig. 10 A selected flight detection Cartesian location comparison with NARX, True and PR syst

Setting the NARX-NN as a closed-loop network to perform multistep predictions, the future values of a time series are predicted from past values of that series, the feedback input, and an external time series. The results were promising, and the research results predicted 100 seconds in the future with an accuracy of 86%. To analyze this result, the error autocorrelation is used (seen in Fig.11), which describes how the prediction errors are related in time. For a better prediction model, there should only be one nonzero value of the autocorrelation function, which should occur at zero lag (the mean square error). This would mean that the prediction errors were completely uncorrelated with each other (white noise). If there was a significant correlation in the prediction errors, then it should be possible to improve the prediction by increasing the number of delays in the tapped delay lines. In this research, the correlations in our data set, except for the one at zero lag, fall approximately within the 95% confidence limits around zero, which means reliable predictions and great improvement in PR systems detection and prediction capabilities.

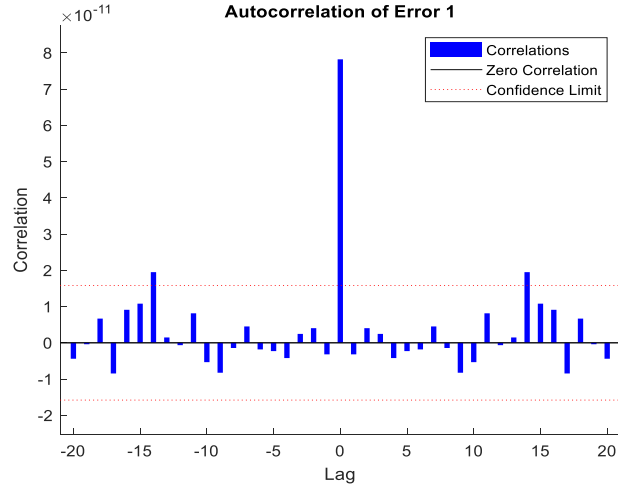


Fig. 11 Autocorrelation of the error in experiment 2

Experiment 2 was repeated with classical SVD decomposing techniques in the second stage for comparison purposes, replacing NARX-NN. The dataset, consisting of 12 million-point recordings coming from more than 5000 flights, was used for the SVD (SVD matrix filter algorithm converts the received signal to a $m \times n$ matrix, reducing the noise value in the signal such that the resultant signal convolves with the transmitted signal). The results showed that the best validation performance was reached at epoch 1050 with MSE=53.7. The SVD algorithm was tested on the same selected flight with 1000 points, resulting in the comparison of both Cartesian and polar plots shown in Fig.12. As can be seen comparing the plots of the SVD, NARX-NN, classical PR system prediction and the ADSB true location, the SVD performance is clearly less accurate than NARX-NN. SVD capabilities are not comparable to NARX-NN in target location, which is a stronger locator because it is a recurrent neural network that relies on accumulated historic target locations previously collected, making it a better choice for the detection of moving objects. With this comparison, it is notable that NARX-NN produces more reliable results with 75% improvement in PR detection compared to the 68% improvement scored by the SVD algorithm; hence, NARX-NN is more recommended to improve target localization of PR systems.

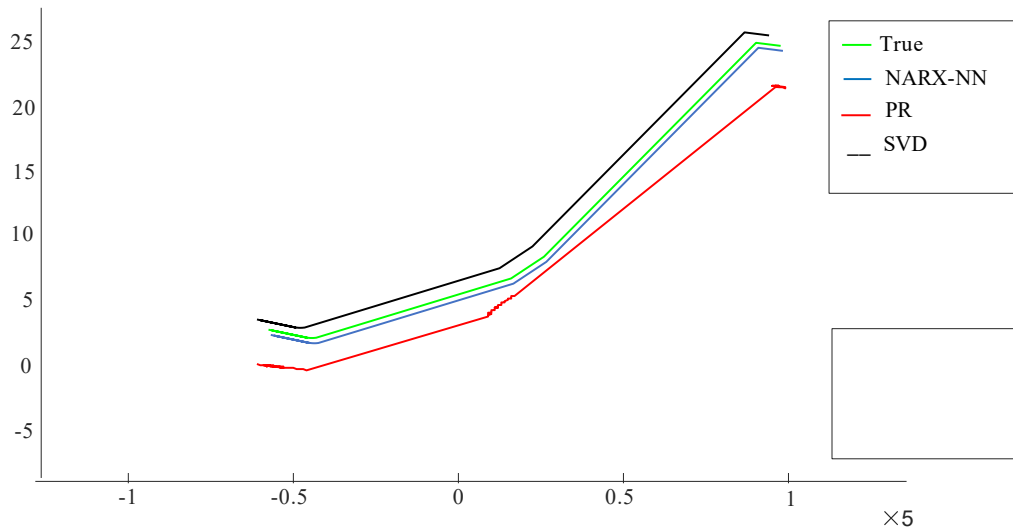


Fig. 12 A selected flight detection Cartesian location comparison with SVD, NARX, True and PR systems

7. Conclusion

In this study, the benefit of Artificial Intelligence techniques in improving the performance of Passive Radar technology is explored. This research relied on the synergy and strength of the backpropagation neural network and the NARX time series' recurrent neural networks. The first stage of this methodology incorporated the Backpropagation ANN to improve the Azimuth measurement, which has been proven to be a key player in improving PR performance. The second stage consisted of using this

improved Azimuth value in the NARX time series Recurrent NN to predict the target location. Recurrent NARX-NN has been shown to be very effective in capturing the dynamic aspects of moving data and time dependency, such as inflight detection problems. The testing results with a new unseen flight were promising and gave a 75% improvement in the PR target detection compared to classical SVD and geometrical PR systems. Hence, this recommendation is for adding NARX-NN and BP-NN algorithms to the PR system as a built-in feature, which will improve target detection and allow the system to learn from past flights and produce more accurate detection.

The research field for improving PR technology is important and still needs more researchers to investigate in order to reach more accurate, reliable target detection, which is very important in aviation surveillance and homeland security. Moreover, future research should investigate more ANN designs and architectures to investigate the interplay of other parameters such as PR range, PR bistatic range and velocity, which may uncover more inter-relations and correlations to their effect on PR systems' performance.

Acknowledgment

All authors thank Prince Sultan Defence Studies and Research Center for Data collection and expert opinion on Passive radar technology.

References

- [1] Mateusz Malanowski, *Signal Processing for Passive Bistatic Radar*, Artech House publishing, 2019. [[Google Scholar](#)] [[Publisher Link](#)]
- [2] Wen-Qin Wang, and Huaizong Shao, "Azimuth-Variant Signal Processing in High-Altitude Platform Passive SAR with Spaceborne/Airborne Transmitter," *Remote Sensing*, vol. 5, no. 3, pp. 1292-1310, 2013. [[CrossRef](#)] [[Google Scholar](#)] [[Publisher Link](#)]
- [3] Xiao Yong Lyu, and Jun Wang, "Direction of Arrival Estimation in Passive Radar Based on Deep Neural Network," *IET Signal Processing*, vol. 15, no. 9, pp. 612-621, 2021. [[CrossRef](#)] [[Google Scholar](#)] [[Publisher Link](#)]
- [4] Li Song, Wang Shengli, and Xie Dingbao, "Radar Track Prediction Method Based on BP Neural Network," *The Journal of Engineering*, vol. 2019, no. 21, pp. 1-5, 2019. [[CrossRef](#)] [[Google Scholar](#)] [[Publisher Link](#)]
- [5] Mohammed Khalafalla et al., "Two-Dimensional Target Localization Approach via a Closed-Form Solution Using Range Difference Measurements Based on Pentagram Array," *Remote Sensing*, vol. 16, no. 8, pp. 1-18, 2024. [[CrossRef](#)] [[Google Scholar](#)] [[Publisher Link](#)]
- [6] Ali Noroozi, and Mohammad Ali Sebt, "Target Localization in Multistatic Passive Radar Using SVD Approach for Eliminating the Nuisance Parameters," *IEEE Transactions on Aerospace and Electronic Systems*, vol. 53, no. 4, pp. 1660-1671, 2017. [[CrossRef](#)] [[Google Scholar](#)] [[Publisher Link](#)]
- [7] Yulong Gao et al., "Gridless 1-b DOA Estimation Exploiting SVM Approach," *IEEE Communications Letters*, vol. 21, no. 10, pp. 2210-2213, 2017. [[CrossRef](#)] [[Google Scholar](#)] [[Publisher Link](#)]
- [8] A.H. El Zooghby, C.G. Christodoulou, and M. Georgiopoulos, "A Neural Network-Based Smart Antenna for Multiple Source Tracking," *IEEE Transactions on Antennas and Propagation*, vol. 48, no. 5, pp. 768-776, 2000. [[CrossRef](#)] [[Google Scholar](#)] [[Publisher Link](#)]
- [9] Zhang-Meng Liu, Chenwei Zhang, and Philip S. Yu, "Direction-of-Arrival Estimation Based on Deep Neural Networks with Robustness to Array Imperfections," *IEEE Transactions on Antennas and Propagation*, vol. 66, no. 12, pp. 7315-7327, 2018. [[CrossRef](#)] [[Google Scholar](#)] [[Publisher Link](#)]
- [10] R.D. DeGroat, E.M. Dowling, and D.A. Linebarger, "The Constrained MUSIC Problem," *IEEE Transactions on Signal Processing*, vol. 41, no. 3, pp. 1445-1449, 1993. [[CrossRef](#)] [[Google Scholar](#)] [[Publisher Link](#)]
- [11] Laurene V. Fausett, *Fundamentals of Neural Networks Architectures, Algorithms and Applications*, Wiley, 1995. [[Google Scholar](#)] [[Publisher Link](#)]
- [12] Bogdan Wiliamowski, and Hao Yu, "Improved Computation for Levenberg-Marquardt Training," *IEEE Transactions on Neural Networks and Learning Systems*, vol. 21, no. 6, pp. 930-937, 2010. [[CrossRef](#)] [[Google Scholar](#)] [[Publisher Link](#)]
- [13] D. Ashok Kumar, and S. Murugan, "Performance Analysis of NARX Neural Network Backpropagation Algorithm by Various Training Functions for Time Series Data," *International Journal of Data Science*, vol. 3, no. 4, pp. 308-325, 2018. [[CrossRef](#)] [[Google Scholar](#)] [[Publisher Link](#)]
- [14] Semra Çoruh et al., "The Use of NARX Neural Network for Modeling of Adsorption of Zinc Ions Using Almond Shell as a Potential Biosorbent," *Bioresource Technology*, vol. 151, pp. 406-410, 2014. [[CrossRef](#)] [[Google Scholar](#)] [[Publisher Link](#)]
- [15] Tsung-Nan Lin et al., "A Delay Damage Model Selection Algorithm for NARX Neural Networks," *IEEE Transactions on Signal Processing*, vol. 45, no. 11, pp. 2719-2730, 1997. [[CrossRef](#)] [[Google Scholar](#)] [[Publisher Link](#)]